

Dark Matter Annihilations in the Causal Diamond

Andrew Scacco and Andreas Albrecht
University of California at Davis; Department Of Physics
One Shields Avenue; Davis, CA 95616
(Dated: February 15, 2022)

We investigate the implications of dark matter annihilations for cosmological parameter constraints using the causal entropic principle. In this approach cosmologies are weighted by the total entropy production within a causally connected region of spacetime. We calculate the expected entropy from dark matter annihilations within the causal diamond and investigate the preferred values of the cosmological constant and the mass and annihilation cross section of the annihilating dark matter and their dependence on the assumptions in the models. For realistic values of the cross section we typically find preferred values of Λ on the order of 10^{-5} of the present value assuming dark matter annihilations are the primary source of entropy production. The greatest amount of entropy production from dark matter within the causal diamond is likely to occur with light keV scale dark matter with low annihilation cross section. We also investigate the effect of combining this entropy with the entropy production from stars, and show that if the primary source of entropy production is from stars, varying the dark matter cross section directly produces a preferred value of Ω_m in excellent agreement with observations.

CONTENTS

I. Introduction	1
II. Entropy in the causal diamond	2
III. Calculation details	3
A. The causal diamond	3
B. Power spectrum of the dark matter	4
C. Halo model and concentration mass relation	5
D. Flux multiplier and linear theory before halos collapse	6
E. Sheth-Tormen formalism	6
F. Total annihilation	7
G. Entropy per annihilation	7
IV. Cross section	8
V. Numerical methods	8
VI. Results	8
A. Entropy in the causal diamond	9
B. Assuming our current value for Λ	10
C. Combining with stars	10
D. Varying the cross section	11
VII. Conclusions	11
Acknowledgments	12
References	13

I. INTRODUCTION

A fundamental understanding of physical laws might yield a picture in which the physical constants are fixed from first principles. Alternatively some or all constants could take on a range of values in some meta picture,

making the values we observe an “environmental” feature of physics. This could be due to the existence of a multiverse, in which our universe is but one of many universes that we might be living in. In many of these multiverse theories, it is possible (or at least hoped to be possible) to predict the distribution of possible universes and their likelihoods. In this case, predictions about values of constants in the universe should boil down to probability distributions, which we could compare with observations using the usual statistical tools. A famous example of this later approach was used by Weinberg to predict a small but positive value for cosmological constant [1] before something like that was observed. This result (and subsequent extensions motivated by the string theory landscape [2]), has generated considerable interest to this approach. Such analysis usually requires some sort of “anthropic” reasoning which folds in some measure of the likelihood of observers existing with different physical parameters. In general, stating exactly what such conditions might be is tricky. Bousso et al. [3] proposed the causal entropic principle (CEP), an elegant approach which weighs different parameter choices according to entropy production in the corresponding cosmology. Entropy increase (the 2nd law) is a critical resource for any imaginable observer, even ones extremely different from us. So entropy production seems to have something to do with counting observers, yet it also is a familiar quantity that physicists are used to calculating in concrete terms.

These methods require entropy production to be measured in a specific four-volume. For the CEP, this volume is the causal diamond, as shown in Fig. 1. The calculation of this volume is given in Sec. III A.

The causal entropic principle (CEP) has been used to find probability distributions for the cosmological constant, curvature, density contrast, baryon fraction, overall matter abundance, and decays of dark matter [4, 5]. Subtleties connected to inhomogeneities have also been pointed out in [6]. Other work on the CEP can be found

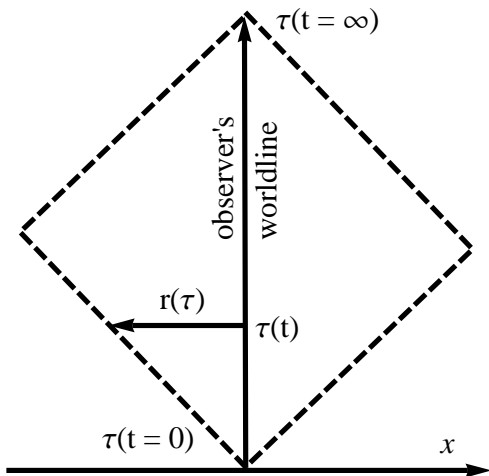


FIG. 1. The causal diamond can be simply described as containing everything that an observer can affect, which in turn can be later observed by that same observer. So the boundaries are the future light cone of the beginning of the observer's worldline and the past light cone of the end of the observer's worldline.

in [7–15].

The new work presented in this paper adds entropy production from dark matter annihilations to the CEP calculations. We calculate the joint probability distribution for dark matter particle mass and Λ , and show that (depending on parameters) dark matter annihilations can significantly impact the results. We discuss several interpretations, including predicting a preferred value of the dark matter particle mass of order 1 keV if Λ is fixed to the observed value. We find our work all the more timely due to recent hints that suggest the possibility of detecting signatures from dark matter annihilations from gamma ray lines, as in [16]. There are tantalizing hints that dark matter annihilations may have been seen by PAMELA [17], ATIC [18], Fermi [19], or AMS [20]. It should be noted, however, that the typical dark matter particles hypothesized to account for these lines are WIMPS at the GeV scale. For simplicity we have chosen a specific family of dark matter models for this work. They are sterile neutrino models which as it happens have been most systematically studied for keV scale dark matter masses. We include extrapolations of these models to GeV scales (which end up being disfavored). Our extrapolated models are not the same as many models currently being proposed in response to these experimental hints, but we expect their general properties to be quite representative for our purposes.

The dark matter particle mass comes in in two important ways. Firstly, in standard thermal production scenarios the dark matter mass is related to the dark matter particle velocities and thus determines the “streaming length” on which cosmic structure is washed out by dark matter motions. Here we consider a range of parameters which run from “cold dark matter” for which the

streaming length is so small as to be unimportant for our considerations as well as “warm dark matter” where the streaming affects some smaller scale aspects of cosmic structure (an advantage, some argue, in providing consistency with observations [21]). Additionally, there are more particles per unit mass for lighter (warmer) dark matter, meaning they will be more likely to find each other to annihilate. Also, since warm dark matter disrupts formation of structures on small scales, the balance of these effects allows for the prediction of the dark matter mass.

II. ENTROPY IN THE CAUSAL DIAMOND

In this section we present a high level overview of the calculation of the entropy produced in the causal diamond and how to calculate the likelihood of a given universe using the prior probability. This section also serves as an outline for later sections which describe our calculations in more detail.

Dark matter can annihilate when two dark matter particles find each other. As such, the dark matter annihilates with greater probability in regions of larger dark matter density. The equation that governs this interaction is given in [22] as

$$\frac{dN_{ann}}{dt} = -\frac{\langle\sigma v\rangle}{m_\chi^2} \int_V \rho^2 dV, \quad (1)$$

where V is the volume, which when applied to the CEP is taken to be the volume of the causal diamond at a given time slice, ρ is the mass density, N_{ann} is the total number of dark matter particles that annihilate within that volume, and m_χ is the mass of the dark matter particle.

For the entropy production from dark matter annihilations,

$$S = g_s N_{ann}, \quad (2)$$

where S is the total entropy production in the causal diamond, g_s is the entropy increase per annihilation, and N_{ann} is the total number of dark matter particles that annihilate within the causal diamond.

The total entropy production within the causal diamond is then

$$S = g_s \int \int \frac{\langle\sigma v\rangle}{m_\chi^2} \rho^2 dV dt \quad (3)$$

$$S = g_s \int \int \frac{\langle\sigma v\rangle}{m_\chi^2} \rho^2 \frac{dV}{dN} \frac{dN}{dM} dM dt \quad (4)$$

$$S = g_s \int \int \frac{\langle\sigma v\rangle}{m_\chi^2} \rho^2 \frac{M}{\rho_{halo}} \frac{dN}{dM} dM dt, \quad (5)$$

where N is the number of dark matter halos, M is the mass of the halo, ρ_{halo} is the average density of the dark matter halo, and the halo is taken to end at its virial radius.

Defining $\Delta \equiv \frac{\rho_{\text{halo}}}{\rho_m}$, where ρ_m is the average matter density in the universe, we obtain

$$S = g_s \int \int \frac{\langle \sigma v \rangle}{m_\chi^2} \rho^2 V \frac{1}{\Delta} \frac{dF}{dM} dM dt, \quad (6)$$

where F is the total fraction of the causal diamond's mass in halos of mass greater than M . Equation 6 can be rewritten as

$$S = g_s \int \int \frac{\langle \sigma v \rangle}{m_\chi^2} \rho_m^2 f V_{\text{com}} a^3 \frac{dF}{dM} dM dt \quad (7)$$

$$\rho_m = \frac{3H_0^2 \Omega_{m,0} a^{-3}}{8\pi G} \quad (8)$$

$$f \equiv \frac{\int \rho^2 dV_{\text{halo}}}{\Delta V_{\text{halo}} \rho_m^2}, \quad (9)$$

where a is the cosmic scale factor, V_{com} is the comoving volume of the causal diamond at fixed time, f is the "flux factor", and V_{halo} is the volume of a halo of mass M .

According to the causal entropic principle, the probability of a parameter having a certain value is proportional to the entropy produced in the causal diamond multiplied by the prior probability on that parameter. For example, taking the parameter in question to be the cosmological constant Λ gives

$$P \propto P(U|\Lambda)P(\Lambda), \quad (10)$$

where P is the probability of observing a cosmological constant Λ . The quantity $P(\Lambda)$ is the prior probability on Λ , and $P(U|\Lambda) = S$ is the probability of observing a universe, given a specific value of Λ , which is equal to the weight factor, which within the causal entropic principle is the total entropy produced in the causal diamond.

Following [3] we take

$$\frac{dP(\Lambda)}{d \log \Lambda} = \Lambda \frac{dP(\Lambda)}{d\Lambda}, \quad (11)$$

where $\frac{dP(\Lambda)}{d\Lambda}$ is a constant. So,

$$\frac{dP}{d \log \Lambda} \propto \Lambda S. \quad (12)$$

In this paper we assume that the velocity averaged cross section $\langle \sigma v \rangle$ is independent of the halo mass M . This need not be true in general, and specifically for the case of Sommerfeld enhancement, halos with low velocity dispersion will have boosted annihilation rates. However, our assumption will simplify the calculations, and we take $\langle \sigma v \rangle$ outside the integrals giving

$$P \propto \Lambda S = \Lambda g_s \frac{\langle \sigma v \rangle}{m_\chi^2} \left(\frac{3H_0^2 \Omega_{m,0}}{8\pi G} \right)^2 \int \int f V_{\text{com}} a^{-3} \frac{dF}{dM} dM dt. \quad (13)$$

The details of how to evaluate this expression are given in Sec. III. This expression is valid for the case in which the quantity of dark matter that has annihilated is small compared to the total quantity of dark matter. The final expression in the more general case even when the quantity of dark matter that has annihilated grows large is presented in Sec. III F and is the expression used in all numeric computations.

III. CALCULATION DETAILS

In this section we cover the details of the assumptions and models used to calculate the total entropy produced within the causal diamond. Most of these are standard treatments, with the exception of Secs. III F and III G.

A. The causal diamond

In the CEP, only annihilations that occur within the causal diamond will contribute to the entropy relevant for predicting parameters in our universe. Thus we must determine the volume of the causal diamond.

The first step is to find the scale factor as a function of time. We utilize the prescription for normalizing the scale factor from Bousso et al. [3], which requires the scale factor to be the same for all choices of cosmological constant in the limit of early time when the cosmological constant is negligible. We use a set of cosmological parameters consistent with the latest results from Planck [23]. Furthermore, we rescale the scale factor, a , so that it is equal to one for the current value of Ω_Λ , $\Omega_{\Lambda,0} \approx 0.68$. We assume a flat universe containing only matter and the cosmological constant. We also use $\Omega_{m,0} = 0.32$, $\Omega_B = 0.049$, $n_s = 0.96$, and $\sigma_8 = 0.83$. The above choices give

$$a = \frac{\sqrt[3]{\Omega_{m,0}} \sinh^{\frac{2}{3}} \left(\frac{3}{2} \sqrt{\Omega_\Lambda} H_0 t \right)}{\sqrt[3]{\Omega_\Lambda}}. \quad (14)$$

where the value of the Hubble constant today is $H_0 = 100h \frac{\text{km/s}}{\text{Mpc}}$, where $h \approx 0.67$. In this form, what we call Ω_Λ can be greater than 1, it is merely proportional to Λ and in our universe matches our value of $\Omega_{\Lambda,0}$. This is acceptable since we cannot define a current time in any universe other than our own. We choose this to make sense only for our universe because it makes it more expedient to extrapolate data. An equivalent and more conceptually pleasing form (that does not have a quantity $\Omega_\Lambda > 1$) is

$$a = \left(\frac{100 \frac{\text{km/sec}}{\text{Mpc}} \sqrt{3\omega_{m,0}} \sinh \left(\frac{1}{2} \sqrt{3\Lambda} t \right)}{\sqrt{\Lambda}} \right)^{\frac{2}{3}}. \quad (15)$$

where $\omega_{m,0} = \Omega_{m,0} h^2$ is the fraction of the critical density comprised of matter density today multiplied by h^2 .

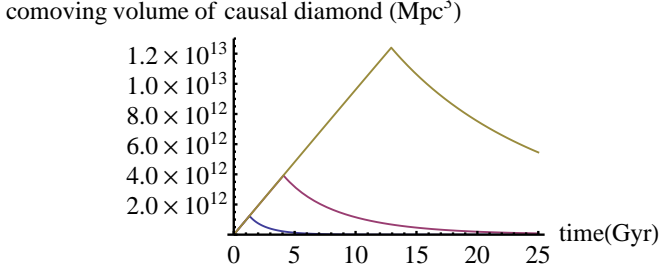


FIG. 2. Comoving volume of the causal diamond as a function of time for various choices of Λ . The top yellow line is for $\Lambda = 10\Lambda_0$, the middle red line is for $\Lambda = \Lambda_0$, and the bottom blue line is for $\Lambda = 0.1\Lambda_0$.

To find the comoving volume of the causal diamond, first we find the conformal time, τ .

$$\tau = \int_0^t \frac{dt}{a} = \int_0^a \frac{da}{a^2 H} \quad (16)$$

$$\tau = -\frac{{}_2F_1\left(\frac{1}{3}, \frac{1}{2}, \frac{4}{3}, -\frac{\Omega_{m,0}}{a^3 \Omega_\Lambda}\right)}{a H_0 \sqrt{\Omega_\Lambda}} \quad (17)$$

where ${}_2F_1$ denotes the Gaussian hypergeometric function.

Next we calculate the radius r of the sphere enclosing the causal diamond at a given time slice, and then hence the comoving volume of the causal diamond, V_{com} on that slice:

$$\Delta\tau = \tau(\infty) - \tau(0) = \frac{\Gamma\left(\frac{1}{6}\right)\Gamma\left(\frac{4}{3}\right)}{\sqrt{\pi}\sqrt{\Omega_\Lambda}^3\sqrt{\frac{\Omega_{m,0}}{\Omega_\Lambda}}} \quad (18)$$

$$r = \frac{\Delta\tau}{2} - \left| \tau + \frac{\Delta\tau}{2} \right| \quad (19)$$

$$V_{\text{com}} = \frac{4\pi}{3} r^3(\tau) \quad (20)$$

We show the volume of the causal diamond as a function of time for various choices of the cosmological constant in Fig. 2.

B. Power spectrum of the dark matter

In order to annihilate and produce entropy, dark matter particles must first find each other. To calculate how likely this is, we must review how dark matter clusters together. This is measured by the matter power spectrum.

For generality, we use the power spectrum for warm dark matter as given in Zentner and Bullock [24] using the BBKS transfer function [25]. We also employ some approximations from Tegmark et al. [26]. The cold dark matter power spectrum appears as a special case of this form.

The root mean square (rms) matter fluctuation within a sphere of radius R , with a top hat window function,

$W(kR)$, is given by $\sigma(M) = \sqrt{\sigma^2(M)}$ where

$$W(kR) = \frac{3}{(kR)^3} (\sin(kR) - (kR) \cos(kR)) \quad (21)$$

$$\sigma^2(M) = \frac{1}{2\pi^2} \int_0^\infty (W(kR))^2 P(k) k^2 dk \quad (22)$$

$$R = \sqrt[3]{\frac{M}{10^{17} M_\odot}} 60 h^{-1} \text{Mpc}. \quad (23)$$

and $P(k)$ is the matter power spectrum, M_\odot is the mass of the sun, M is the mass of the dark matter halo, and the values of $10^{17} M_\odot$ and $60 h^{-1} \text{Mpc}$ come from WMAP + SDSS data [26]. These fluctuations are given for the present time and assuming that the growth of perturbations is linear. As large scale structure forms, the perturbations become highly nonlinear, and will be modeled using the halo formalism in Sec. III C.

The warm dark matter power spectrum is given by $P_{\text{WDM}}(k) = P_{\text{CDM}}(k) \exp(-k R_f - (k R_f)^2)$, where $P_{\text{CDM}}(k)$ is the cold dark matter power spectrum and R_f is the free streaming scale as given in Zentner and Bullock [24] at which the dark matter particle begins to suppress the growth of structure:

$$P_{\text{CDM}}(k) = 2\pi^2 \left(\frac{c}{H_0}\right)^{3+n} (\delta_H)^2 k^n T(q(k))^2 \quad (24)$$

$$R_f(m_\chi) = 0.11 \text{Mpc} \sqrt[3]{\frac{\Omega_\chi h^2}{0.15}} \left(\frac{m_\chi}{\text{keV}}\right)^{-4/3} \quad (25)$$

$$\Omega_\chi = \Omega_{m,0} - \Omega_B. \quad (26)$$

Here $n \approx 0.96$ is the spectral index, $\delta_H \approx 2 \times 10^{-5}$ is the fluctuation amplitude at horizon crossing, $T(q(k))$ is the BBKS transfer function [25], m_χ is the mass of the dark matter particle, Ω_χ is the fraction of mass density in dark matter compared to the critical density, and $\Omega_B \approx 0.049$ is the fraction of mass density in baryons compared to the critical density:

$$T(q) = \frac{\log(1 + 2.34q)}{2.34q} \times \quad (27)$$

$$(1 + 3.89q + (16.1q)^2 + (5.46q)^3 + (6.71q)^4)^{-\frac{1}{4}} \quad (28)$$

$$q(k) = \frac{k}{\Omega_{m,0} h^2 \exp\left(-\Omega_B - \frac{\Omega_B}{\Omega_{m,0}}\right)}$$

Examples of these warm dark matter $\sigma(M)$ functions are shown in Fig. 3.

This set of equations is valid for the rms mass fluctuations today. In order to convert to fluctuations at other times, we simply multiply by the growth factor of linear perturbations, $D(a)$:

$$\sigma(M, a, \Lambda) = \sigma(M) D(a, \Lambda). \quad (29)$$

For a flat universe consisting of only matter and a cosmological constant, the growth factor has an analytic so-

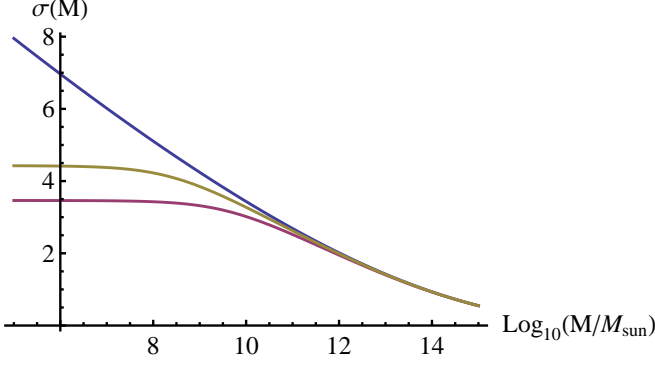


FIG. 3. Warm dark matter $\sigma(M)$ functions for two choices of the dark matter mass. The top blue line is for the cold dark matter model using the BBKS transfer function [25], and the bottom red and middle yellow lines are for dark matter masses of 1 and 2 keV, respectively.

lution

$$D(a, \Lambda) = a \frac{{}_2F_1\left(\frac{1}{3}, 1; \frac{11}{6}; -\frac{a^3 \Omega_\Lambda}{\Omega_{m,0}}\right)}{{}_2F_1\left(\frac{1}{3}, 1; \frac{11}{6}; -\frac{\Omega_{\Lambda,0}}{\Omega_{m,0}}\right)}. \quad (30)$$

We have normalized the growth factor, $D(a, \Lambda)$, to be equal to 1 at the present time in our universe. Specifically, $D(1, \Lambda_0) = 1$.

For the purpose of numerical computation, we would like to have a function for $\sigma(M)$ that does not have to be integrated every time it is used. We use the fitting formula of Tegmark et al. [26], and cut off $\sigma(M)$ at a maximum value, σ_{\max} , the maximum value $\sigma(M)$ attains as $M \rightarrow 0$:

$$\sigma_{\max} = \sqrt{\frac{1}{2\pi^2} \int_0^\infty P(k) k^2 dk}. \quad (31)$$

The scale-dependence of $\sigma(M)$, $s(\mu)$, is approximately given by Tegmark et al. [26] as

$$s(\mu) \approx \left[(9.1\mu^{-\frac{2}{3}})^\beta + (50.5 \log_{10}(834 + \mu^{-\frac{1}{3}}) - 92)^\beta \right]^{1/\beta}, \quad (32)$$

where $\beta = -0.27$, and $\mu = \xi^2 M$, where $\xi^2 = \frac{1}{10^{17} M_\odot}$. This leads to a fit to the cold dark matter $\sigma(M)$

$$\sigma_0(M) \approx 0.2 \frac{\xi^{4/3}}{\rho_\Lambda^{1/3}} \delta_H s(\mu), \quad (33)$$

where Planck units are used, and where ρ_Λ is the energy density of the cosmological constant.

Modified with the cutoff for σ_{\max} , we obtain a good fit with the ansatz

$$\sigma(M) = \sigma_{\max} \left(1 - e^{-\left(\frac{\sigma_0(M)}{\sigma_{\max}}\right)^4} \right)^{1/4}. \quad (34)$$

C. Halo model and concentration mass relation

The greatest number of dark matter annihilations will occur in regions in which the dark matter density is largest. These regions are dark matter halos. We use the NFW model [27] for the density profiles of the halos, and the model of Bullock et al. [28] with the cosmology dependence of Dolag et al. [29] for the concentration mass relation.

The NFW profile is a widely used model for the density profiles of dark matter halos, with a formally infinite mass which is cut off at the virial radius, and divergent central density. The NFW profile is given by

$$\rho(r) = \frac{\rho_s}{\frac{r}{r_s} \left(1 + \left(\frac{r}{r_s} \right)^2 \right)}, \quad (35)$$

where $\rho(r)$ is the density, r_s is the scale radius of the halo, and ρ_s is twice the density at the scale radius.

We define the concentration parameter and the virial radius to match Bullock et al. [28]

$$c \equiv \frac{r_{\text{vir}}}{r_s} \quad (36)$$

$$\bar{\rho} = \Delta \rho_m \quad (37)$$

$$\Delta \approx 18\pi^2 + 52.8x^{0.7} + 16x \quad (38)$$

$$x \equiv \frac{\Omega_\Lambda}{\Omega_m} = \frac{\Omega_\Lambda}{\Omega_{m,0}} a^3 \quad (39)$$

$$x = \sinh^2 \left(\frac{3}{2} \sqrt{\Omega_\Lambda} H_0 t \right), \quad (40)$$

where c is the concentration ratio of the halo, r_{vir} is the virial radius of the halo, $\bar{\rho}$ is the average halo density within the virial radius, and Δ is defined as the ratio of the average halo density within the virial radius to the average density of the universe which we have approximated using the prescription of Tegmark et al. [26].

Now it remains to calculate the clustering properties of the dark matter halos. We will use the model of Bullock et al. [28] for the concentration mass relation. Halos are assumed to have been formed with a NFW profile and a concentration of 3.5, when halos of 1/1000 of the mass of the halo would have been collapsing.

Bullock et al. define the scale factor of collapse a_c as the epoch at which the typical collapsing mass, $M_*(a_c)$, equals a fixed fraction F of the halo mass at epoch a ,

$$M_*(a_c) \equiv F M_{\text{vir}}. \quad (41)$$

Using the spherical collapse model, the scale factor a at which typical halos are collapsing is defined by $\sigma[M_*(a)] = 1.686/D(a)$, where $\sigma(M)$ is the $a = 1$ linear rms density fluctuation on the comoving scale encompassing a mass M , and $D(a)$ is the linear growth rate.

Dolag et al. [29] consider concentration ratios in alternative dark energy cosmologies. They find that the concentration mass relation should be modified by introducing an extra factor of $\frac{D(a)}{D_{\Lambda\text{CDM}}(a)}$. Using also their best

fit parameters for the model of Bullock et al. [28], we obtain

$$c(M, \Lambda, a) = 3.5 \frac{a}{a_{\text{coll}}} \frac{D(a, \Lambda)}{D(a, \Lambda_0)} \quad (42)$$

$$\sigma(0.001M, a_{\text{coll}}) = \delta_c, \quad (43)$$

where $\delta_c = 1.686$ is the linear theory overdensity of collapse. These equations are solved numerically, which gives the concentration ratio for a given mass throughout the history of the universe in each cosmology.

D. Flux multiplier and linear theory before halos collapse

In order to model accurately the actual density squared of the entire universe we must consider not only virialized halos but also obtain a good model for what happens up until the time that they collapse. In this case we use the simple spherical collapse model [30]. To that end, we will calculate the flux factor corresponding to the ratio of annihilation flux that would be produced from the clumpy density profile of space divided by what would be produced if the universe were of perfectly uniform density.

$$f = \begin{cases} \Delta f(c) & \sigma > 1.686 \text{ or } \Delta f(c) < f(\theta) \\ f(\theta) & \text{otherwise} \end{cases} \quad (44)$$

For halos, plugging in the NFW profile, the result we need is

$$f(c) = \frac{1}{\bar{\rho}^2 V} \int_0^{r_{\text{vir}}} \rho(r)^2 4\pi r^2 dr \quad (45)$$

$$\bar{\rho} = \frac{1}{V} \int_0^{r_{\text{vir}}} \rho(r) 4\pi r^2 dr \quad (46)$$

$$f(c) = \frac{c^3 - c^3/(1+c)^3}{9(\ln(1+c) - c/(1+c))^2}, \quad (47)$$

where c is the concentration ratio of the halo, $\bar{\rho}$ is the average density of the halo within the virial radius, and $f(c)$ is the flux multiplier of [22].

For clumps of matter that have yet to virialize and collapse, we have that [30]

$$f(\theta) = 1 + \left(\frac{9(\theta - \sin(\theta))^2}{2(1 - \cos(\theta))^3} - 1 \right)^2 \quad (48)$$

$$\left[\left(\frac{20}{3} \sigma \right)^{3/2} = 6(\theta - \sin(\theta)) \right], \quad (49)$$

where θ is defined by the solution to (49), and $\sigma = \sigma(M, a, \Lambda)$ is the rms matter fluctuation within a sphere of density ρ_m that would enclose the mass of the clump.

E. Sheth-Tormen formalism

In order to predict how much dark matter annihilation occurs in halos, we need to know how many halos there

are for each mass of halo. To do this we utilize the Sheth-Tormen model for obtaining the fraction of halos of a given mass [31]

$$\nu f(\nu) = 2A \left(1 + \frac{1}{\nu^{2q}} \right) \left(\frac{\nu^2}{2\pi} \right)^{1/2} \exp \left(-\frac{\nu^2}{2} \right), \quad (50)$$

where $f(\nu)$ is the distribution function for the fraction of the total mass contained in halos of mass greater than M , $\nu \equiv 1.686/\sigma$, $\sigma = \sigma(M, a, \Lambda)$, $q = 0.3$ and $A \approx 0.3222$.

The quantity that will be useful for our purposes is the fraction dF of the total mass in halos with mass between M and $M + dM$

$$\frac{dF}{dM} = \frac{dF}{d\nu} \frac{d\nu}{d\sigma} \frac{d\sigma}{dM} \quad (51)$$

$$\frac{dF}{d\nu} = A \left(1 + \frac{1}{\nu^{2q}} \right) \left(\frac{2}{\pi} \right)^{1/2} \exp \left(-\frac{\nu^2}{2} \right) \quad (52)$$

$$\frac{d\nu}{d\sigma} = -\frac{1.686}{\sigma^2}, \quad (53)$$

where $\frac{d\sigma}{dM}$ is the derivative of $\sigma(M, a, \Lambda)$ with respect to M .

This formalism works well if we assume that there is no free streaming scale for the dark matter, so that it has the property that all the mass is contained in halos of some size:

$$\int_0^\infty \frac{dF}{dM} dM = 1. \quad (54)$$

But with a cutoff for sigma at low mass scales this no longer works because the rms mass fluctuations cannot go to infinity at small mass scales:

$$\int_0^\infty \frac{dF}{d\sigma} d\sigma = 1 \quad (55)$$

$$\int_0^{\sigma_{\text{max}}} \frac{dF}{d\sigma} d\sigma \neq 1. \quad (56)$$

However, the Sheth-Tormen formalism has been tested and fit by data from large structures in our own universe, where there is no difference between the warm dark matter clustering and the cold dark matter clustering because the matter power spectrum is not yet cut off at those large mass scales. So there is a quantity of matter that simply does not collapse into halos, which we can just use the linear theory results to account for. This becomes more and more the case at earlier times. There is also an effect to be accounted for at large mass scales, since these will never collapse into a halo, even in the infinite future. These objects should be treated according to the linear theory too, since they will not collapse. For a more detailed treatment of warm dark matter clustering, see [32–34].

For our purposes, we are concerned with the largest sources of annihilation, which are those dense halos which annihilate rapidly, for which there is no conflict. This will in fact be overwhelmingly larger than the contribution from annihilations in regions that do not clump to form

halos. At early times when the smooth not yet clumped together portion becomes large, the total amount of annihilation in the causal diamond becomes very small. Thus we expect our neglect of this issue to have little effect on the results.

F. Total annihilation

Up until this point, we have assumed that the annihilation of dark matter does not have any feedback effect on the density profiles of halos. But as more and more dark matter annihilates at late times, eventually so much will have annihilated that it will become an appreciable fraction of the total dark matter particles available to annihilate and annihilation will slow down. This is very important since it cuts off the otherwise potentially (formally) unbounded amount of annihilation at late times.

We model this in a very simple way by assuming that for each mass scale of halo there is some maximum number of annihilations that can occur, and that furthermore, these annihilations modify the halo density profile only by changing the total overall density, and do not heat the halo or slow down the annihilation faster in the more dense central regions where more annihilations occur as would be the case for real halos.

We begin with the Boltzmann equation for annihilation,

$$\frac{dn}{dt} + 3Hn = -\langle\sigma v\rangle (n^2 - n_{eq}^2), \quad (57)$$

where n is the number density of dark matter particles, and $n_{eq} \approx 0$ is the equilibrium number density of dark matter.

On scales of mass M ,

$$\frac{dN}{dt} = -\frac{\langle\sigma v\rangle}{m_\chi^2} \left(\frac{3H_0^2 \Omega_{m,0}}{8\pi G} \right)^2 f a^{-3} \left(\frac{N}{N_{\max}} \right)^2 \quad (58)$$

$$N_{\max} = \frac{\rho_m}{m_\chi} a^3 = \frac{\rho_{m,0}}{m_\chi}, \quad (59)$$

where $N = na^3$, and N_{\max} is the initial value of N , before annihilations from clustering decrease the number density of dark matter particles.

We plot $\log(fa^{-3})$ vs. $\log(a)$ in Fig. 4 and find

$$\log(fa^{-3}) = \beta \log(a) + C, \quad (60)$$

where $\beta \approx 13.4$, and we are far into cosmological constant domination by the time all the dark matter has annihilated. So,

$$a \propto e^{\sqrt{\Omega_\Lambda} H_0 t} \quad (61)$$

$$\frac{dN}{dt} = -\langle\sigma v\rangle f a^{-3} N^2 \quad (62)$$

$$\frac{dN}{N^2} = -\langle\sigma v\rangle e^{C+\sqrt{\Omega_\Lambda} H_0 \beta t} dt \quad (63)$$

$$\frac{1}{N} = \frac{1}{N_{\max}} + \frac{\langle\sigma v\rangle}{\sqrt{\Omega_\Lambda} H_0 \beta} f a^{-3} \quad (64)$$

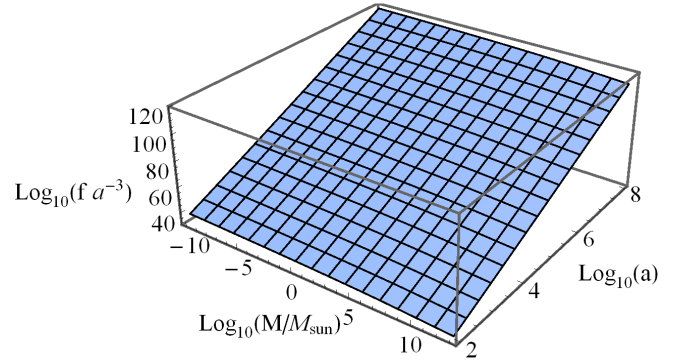


FIG. 4. $\log(fa^{-3})$ vs. $\log(a)$ for the warm dark matter for $\Omega_\Lambda = 0.7$ and $h = 0.7$ and $\Omega_m = 0.3$. This surface can be well approximated by the linear fit $\log(fa^{-3}) = 13.4 \log(a) + 20.7$. The slope of this fit is the same across all choices of parameters and is valid for all mass scales that eventually collapse into halos, in our model, for $\log\left(\frac{M}{M_\odot}\right) < 13.6$.

We then adjust the expression for entropy production within the causal diamond by the ratio of $\left(\frac{N}{N_{\max}}\right)^2$, yielding the final form to go into the numerical computation,

$$P \propto S\Lambda = \Lambda g_s \frac{\langle\sigma v\rangle}{m_\chi^2} \left(\frac{3H_0^2 \Omega_{m,0}}{8\pi G} \right)^2 \int \int f V_{\text{com}} a^{-3} \frac{dF}{dM} \frac{1}{\left(1 + \frac{1}{\sqrt{\Omega_\Lambda} H_0 \beta} \frac{\langle\sigma v\rangle}{m_\chi} \left(\frac{3H_0^2 \Omega_{m,0}}{8\pi G} \right) f a^{-3} \right)^2} dM dt. \quad (65)$$

G. Entropy per annihilation

One of the most important parameters governing how much entropy is produced by dark matter annihilations is the amount of entropy produced by each dark matter

annihilation, g_s . This in general depends on both the particle physics model for the annihilation and the astrophysical details of how the end state particles thermalize. If the dark matter produces photons that eventually scatter off dust particles like in the case of ordinary starlight, the entropy per annihilation is proportional to the energy

of the dark matter particle. If the dark matter annihilates to neutrinos that do not later interact, the entropy per annihilation will be a constant.

At this stage in our understanding of dark matter, we find it more convenient to just assume the simple functional form of a power law for the dependence of the expected entropy produced per dark matter annihilation as a function of the mass of the dark matter particle¹:

$$g_s = g_0 \left(\frac{m_\chi}{\text{keV}} \right)^\gamma, \quad (66)$$

where g_0 is the entropy per annihilation of a 1 keV dark matter particle, and we have introduced γ as the parameter determining the dependence on mass. This parameterization allows us explore the predictions of which values of dark matter mass are favored as a function of γ and g_0 .

IV. CROSS SECTION

The cross section for annihilation will affect both the initial abundance of dark matter, and the later annihilation rate. In all sections except Sec. VID, we hold the matter density fixed at $\Omega_m = 0.32$, in order that the fitting functions derived from observations and simulations will be accurate. In Sec. VID, we explore the effect of varying the cross section for dark matter annihilation on the total entropy production. We assume that the same cross section that governs annihilation in the early universe holds in the late universe as well. We solve the Boltzmann equation numerically as in [35] to obtain the initial amount of dark matter, which will determine the baryon fraction, and the matter abundance. Then we use the relations of [4] to adjust the clustering properties of matter. Note that in Sec. VID the fitting functions are still based on simulations of universes with values of the matter density, $\Omega_m \approx 0.32$, a weakness we hope to correct in future work.

V. NUMERICAL METHODS

In this section, we present the details of how the formulas presented earlier were processed numerically to generate the final probability plots.

In performing the calculations, we can calculate the differential entropy production per unit time per unit mass of halo. It is convenient to parameterize time and mass scale logarithmically using

$$M = 10^y \quad (67)$$

$$t = 10^w, \quad (68)$$

¹ Formally, one should think of this formula as the product of the entropy production per particle with the prior probability assigned to a theory with dark matter mass m_χ .

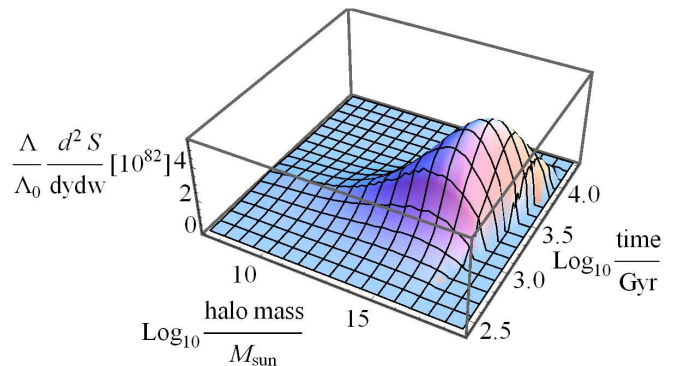


FIG. 5. An example of the integrand of the integral for total entropy plotted over the region in which the integral is significant. In this plot, $\Lambda = 10^{-5}\Lambda_0$ and $m_\chi = 1$ keV. This type of plot shows that this integral to get the total entropy is convergent and also the time and mass scales at which the greatest number of annihilations will occur.

where for convenience, we express time in units of Gyr, and mass in units of solar masses, M_\odot .

Then the task is to integrate Eq. (65) over all time and all mass scales. Our integrations converge nicely thanks to the intrinsically finite physical processes which are being computed. Performing a 2D array of these 2D integrals to get the output plots as a function of Λ and dark matter mass was not overly resource intensive and was done on a laptop.

The time integral converges at the point when when most of the dark matter has already annihilated and the rate slows dramatically. At early times the annihilation rate is very rapidly increasing with time as halos cluster more and more. Early epochs have much less annihilation and so ultimately it is only the final (logarithmic) epoch just before all the dark matter annihilates that dominates the integral.

The cutoff at low mass scales for halos occurs where the free streaming scale of the dark matter particle cuts off structure formation. This can go down to keV ranges with our model until it cuts off almost all structure formation on all scales. The cutoff at high mass scales comes from the Sheth-Tormen formalism. There is a maximum size limit to the size of bound objects that increases with time, so at late times this cutoff is at larger mass scales than at early times. A typical plot of the integrand in the region in which the integral is significant is shown in Fig. 5.

VI. RESULTS

Here we present the results of our calculations. In Sec. VIA we present the probability distribution in Λ - m_χ space that results from only including the entropy produced by dark matter annihilation in the CEP weighting. This limited analysis helps us understand the impact of adding the new (dark matter annihilation) ingredient. In

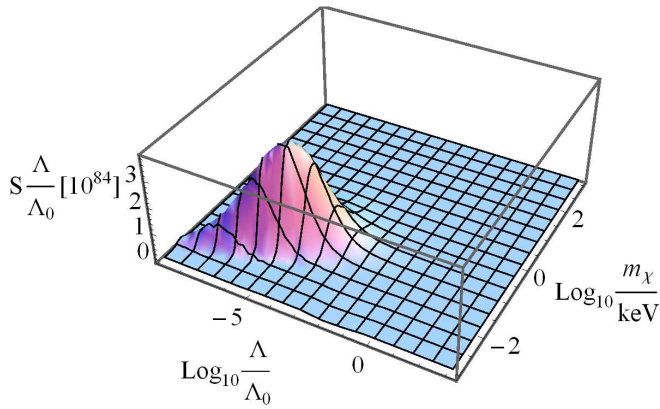


FIG. 6. Probability of observing a given value of the cosmological constant and mass of dark matter, assuming $g_s = 1$, $\langle\sigma v\rangle = 3 \times 10^{-26} \frac{\text{cm}^3}{\text{s}}$, and that dark matter annihilation is the only contributor to entropy production in the causal diamond. The peak of this plot occurs for $\Lambda \approx 9.3 \times 10^{-6} \Lambda_0$ and $m_\chi \approx 0.04 \text{ keV}$.

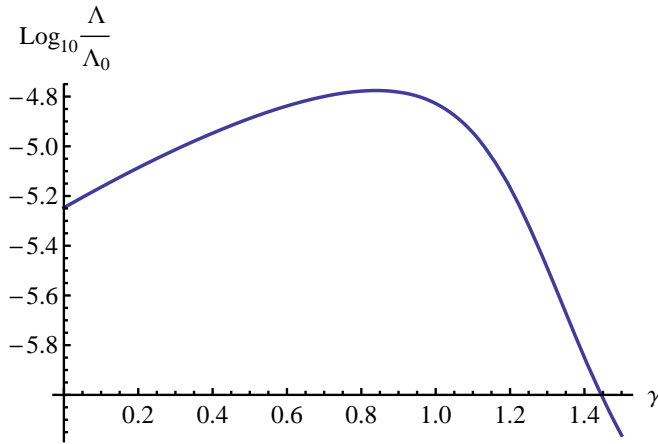


FIG. 7. The expected value of the cosmological constant marginalized over mass of dark matter as a function of the power law index γ for the entropy per annihilation, assuming $g_s \propto m_\chi^\gamma$, and $\langle\sigma v\rangle = 3 \times 10^{-26} \frac{\text{cm}^3}{\text{s}}$. Here only entropy production from annihilations is included, and we neglect entropy production from stars.

Sec. VIB we scrutinize this distribution further by examining a slice at fixed Λ (corresponding to the concordance value). We present results from adding the (usual) stellar burning contribution in Sec. VIC. In Sec. VID we explore the effect of varying the cross section for dark matter annihilation, both on the stellar entropy and the entropy from dark matter annihilation.

A. Entropy in the causal diamond

We obtained the total entropy produced in the causal diamond, due only to dark matter annihilations, as a function of Λ and mass of the dark matter. This is then

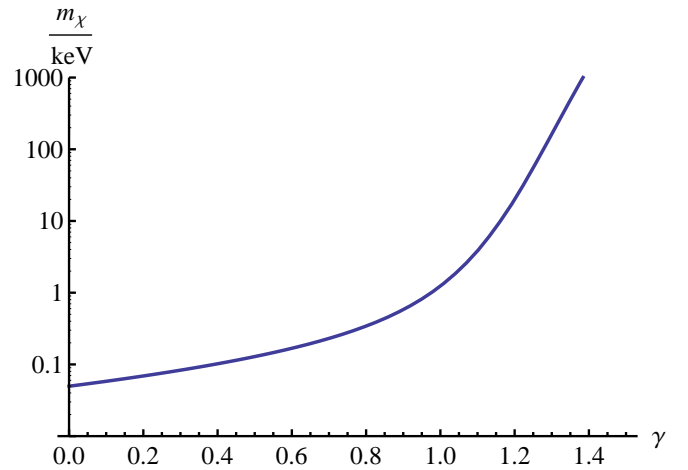


FIG. 8. The expected value of dark matter mass marginalized over the cosmological constant as a function of the power law index γ for the entropy per annihilation, assuming $g_s \propto m_\chi^\gamma$, and $\langle\sigma v\rangle = 3 \times 10^{-26} \frac{\text{cm}^3}{\text{s}}$. Here only entropy production from annihilations is included, and we neglect entropy production from stars.

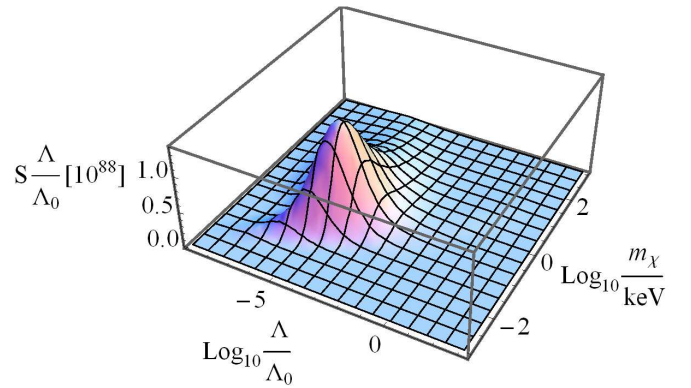


FIG. 9. Probability of observing a given value of the cosmological constant and mass of dark matter, assuming $g_s = \frac{m_\chi}{20 \text{ meV}}$, $\langle\sigma v\rangle = 3 \times 10^{-26} \frac{\text{cm}^3}{\text{s}}$, and that dark matter annihilation is the only contributor to entropy production in the causal diamond. This plot assumes the dark matter annihilates into photons which are scattered by dust at energies of 20 meV. The peak of this plot occurs for $\Lambda \approx 3.2 \times 10^{-5} \Lambda_0$ and $m_\chi \approx 0.14 \text{ keV}$.

weighted by the prior on Λ , which is assumed to be proportional to the value of Λ itself (following the standard approach). A plot of the probability distribution is shown in Fig. 6. Since small values of Λ allow the causal diamond to stay large for a longer period of time, they will produce more entropy than large values do. So the cutoff for Λ occurs where the extra size of the causal diamond at late times does not help gain much more entropy. This typically occurs at the epoch at which a sizable fraction of the dark matter has annihilated. This in general happens in the far future, and leads to the low favored values for Λ , in contrast to traditional CEP calculations (which

model stellar entropy production).

In the dark matter mass direction, low masses allow more annihilations because there are more dark matter particles for the same total dark matter mass, and hence they are more likely to find each other and annihilate. When we vary the power law index γ for the entropy per annihilation in Figs. 7 and 8, we see that a low mass dark matter particle is favored for all $\gamma < 1.4$, and that for higher values of γ , the dark matter is favored to have arbitrarily high mass approaching infinite mass in our crude model with no cutoff for mass. This is because low values of dark matter mass will produce more entropy because their annihilation rate goes as the number density squared, but too low values of the dark matter mass will suppress structure formation too well and will not allow enough annihilation-enhancing halos to form. In general the balance between these effects favors a dark matter mass pushing up against the limit where structure formation is totally cut off, which happens just below the keV scale in our model. If we use the simple model that dark matter annihilations produce light which gets most of its entropy from heating of dust just like ordinary starlight, as in [3], we get the plot presented in Fig. 9. This model produces more peak entropy from dark matter annihilations than would be produced by stars.

The preferred value of the cosmological constant is roughly 10^{-5} times the measured value today, regardless of the value of γ . In general, most of the annihilation of dark matter will occur in the far future as halos continue to collapse more and more.

B. Assuming our current value for Λ

These preferred values of Λ do not agree with the current accepted value for Λ . Using the standard causal entropic principle with entropy from stars predicts agreement within 1 sigma for the cosmological constant. We find a disagreement of at minimum 2 sigma in the opposite direction for all choices of dark matter mass if we assume all the entropy production comes from dark matter annihilation. We find it interesting to assume some other consideration fixes the observed value of Λ (perhaps simply a prior based on current data). We then might still be able to make useful predictions about the favored value of the dark matter mass, by simply assuming the observed value for Λ , rather than letting it vary. We plot the relative probability for dark matter mass fixing Λ to the currently measured value for the model in which energy from dark matter annihilations produces entropy from heating of dust ($\gamma = 1$) in Fig. 10. This peaks at around 1 keV or so, which is an order of magnitude more massive than the peak if Λ is allowed to vary. We can also determine the most likely value for the dark matter mass as a function of γ here too, which we show in Fig. 11. We can see that here the dependence on γ is more mild than in the case where we also allow Λ to vary.

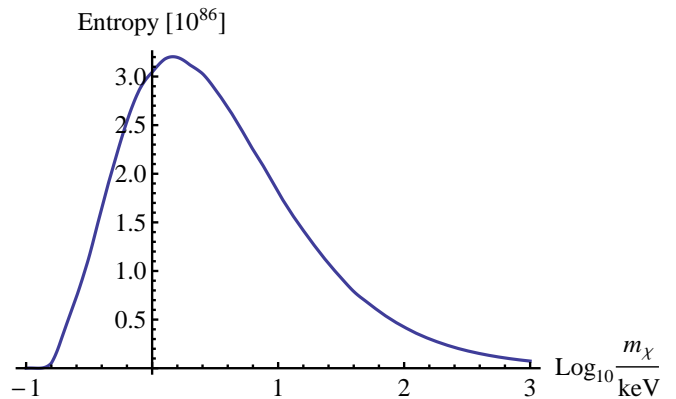


FIG. 10. Probability of observing a given mass of the dark matter particle, fixing the cosmological constant at its current measured value, $\Omega_\Lambda \approx 0.68$, assuming $g_s = \frac{m_\chi}{20\text{meV}}$, $\langle\sigma v\rangle = 3 \times 10^{-26} \frac{\text{cm}^3}{\text{s}}$, and that dark matter annihilation is the only contributor to entropy production in the causal diamond.

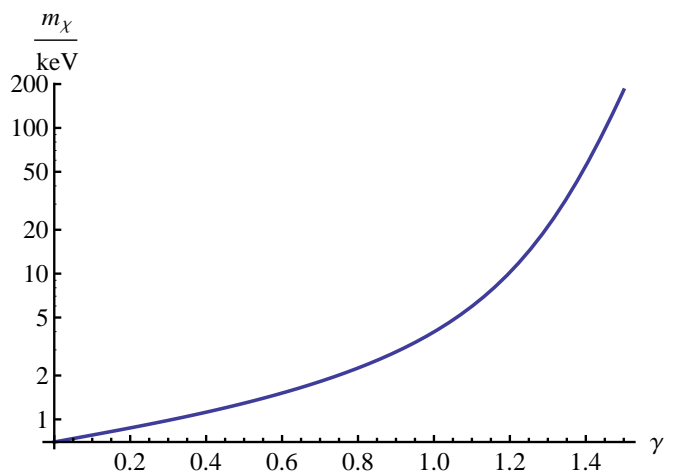


FIG. 11. The expected value of dark matter mass as a function of the power law index γ for the entropy per annihilation, assuming $\Omega_\Lambda = 0.68$, $g_s \propto m_\chi^\gamma$, and $\langle\sigma v\rangle = 3 \times 10^{-26} \frac{\text{cm}^3}{\text{s}}$. Here only entropy production from annihilations is included, and we neglect entropy production from stars.

C. Combining with stars

Dark matter annihilations have the potential to produce a very large amount of entropy within the casual diamond, but do they produce enough entropy to compete with the entropy from dust heated by starlight? Following [4], we add in the contribution from stars, calculated as in Bousso et al. [3], and using the star formation rate of Hernquist and Springel [36], we can see how much entropy per annihilation is needed to shift the predictions, and explore the parameter space of the true solution using both entropy from stars and dark matter annihilation. This contribution is seen to result in two distinct peaks in the probability plot, as shown in Fig. 12. The locations of both peaks have little dependence on each other, since

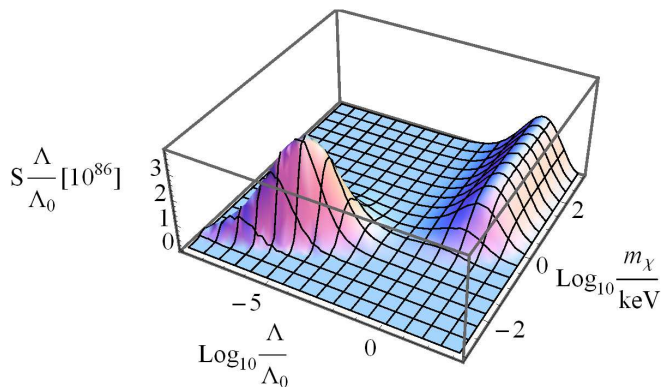


FIG. 12. Probability of observing a given value of the cosmological constant and mass of dark matter, assuming $g_s = 100$, $\langle\sigma v\rangle = 3 \times 10^{-26} \frac{\text{cm}^3}{\text{s}}$, and that both dark matter annihilation and stars contribute to entropy production in the causal diamond. The relative heights of the two peaks depend on the parameters given to the dark matter model.

there was likely little dark matter annihilation during the epoch of peak star formation and there will be little star formation in the epoch where the peak of dark matter annihilation is calculated to occur. So, the value of the cosmological constant predicted from this combined approach is either the value obtained as in Bouusso et al. [3], or the value optimized by the dark matter annihilation obtained here, depending on which regime dominates the probability. We note that while the preferred values for Λ found in [3] were on the high side, and the dark matter annihilations prefer low Λ 's, mixing the two produces a bimodal probability distribution, not a single shifted peak. So our result does not offer a simple way to tune the preferred value (which in any case is not too far off the observed value in the limit when either effect dominates).

D. Varying the cross section

We can add in the effect of varying the cross section for dark matter annihilation to the results. Firstly, if we consider the effect of varying the dark matter annihilation cross section on the entropy produced from stars, this will directly influence the total quantity of dark matter. If we vary the quantity of dark matter directly, we see that the combined effect on both the matter abundance and baryon fraction results in a preferred value of Ω_m in excellent agreement with the observed value as shown in Fig. 13. While [4] vary both the matter abundance and baryon fraction separately, we get better agreement than they do when we vary the dark matter cross section holding baryonic physics fixed, which we believe is more physically motivated.

When we vary the cross section, we notice that the effect of increasing the matter abundance is to cause the dark matter to cluster earlier. The probability of observ-

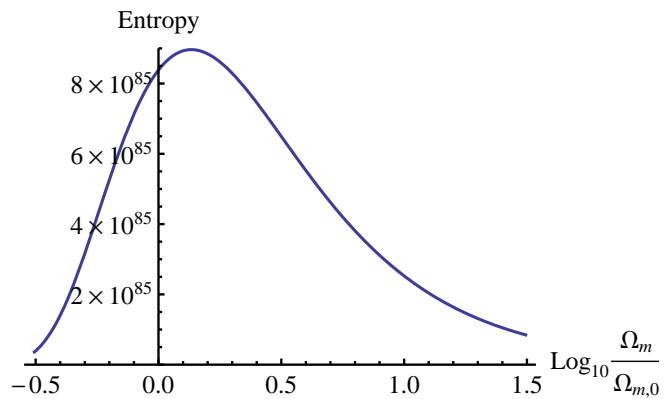


FIG. 13. Probability of observing a given value of the overall matter abundance, by varying the cross section of dark matter annihilation, and holding fixed baryonic physics, assuming stellar entropy dominates over entropy from dark matter annihilations in the causal diamond.

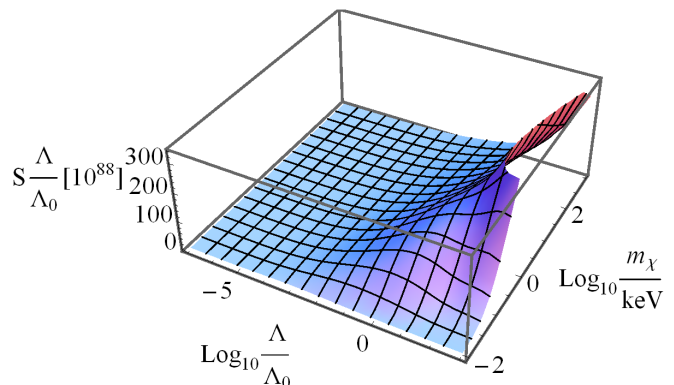


FIG. 14. Probability of observing a given value of the cosmological constant and mass of dark matter, assuming $g_s = \frac{m_\chi}{20 \text{ meV}}$, $\langle\sigma v\rangle = 3 \times 10^{-28} \frac{\text{cm}^3}{\text{s}}$, and that dark matter annihilation is the only contributor to entropy production in the causal diamond. This plot assumes the dark matter annihilates into photons which are scattered by dust at energies of 20 meV.

ing a universe is maximized when the peak of dark matter annihilation matches the peak of the volume of the causal diamond, so with more matter abundance, the earlier clustering allows us to pick a larger cosmological constant, with roughly the same total entropy production, yielding a runaway preference for huge matter densities as found in [13], and shown in Figs. 14, 15, 16, and 17. This runaway behavior would suggest that our universe is extremely unlikely; however, as pointed out in [4], this could be cut off by the formation of black holes which would hide the entropy behind the horizon.

VII. CONCLUSIONS

Our calculations have led to these important points to take away. First, it appears that light keV scale dark

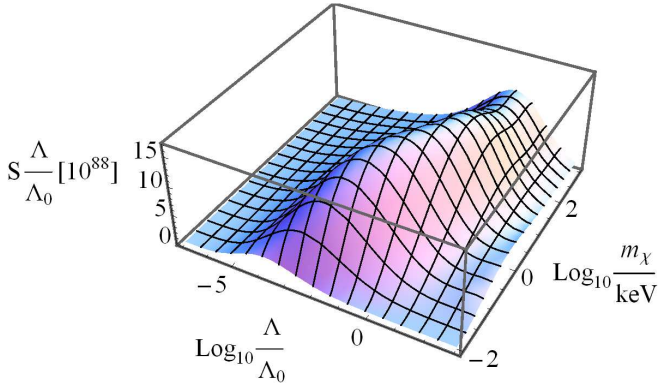


FIG. 15. Probability of observing a given value of the cosmological constant and mass of dark matter, assuming $g_s = \frac{m_\chi}{20\text{meV}}$, $\langle\sigma v\rangle = 3 \times 10^{-27} \frac{\text{cm}^3}{\text{s}}$, and that dark matter annihilation is the only contributor to entropy production in the causal diamond. This plot assumes the dark matter annihilates into photons which are scattered by dust at energies of 20 meV.

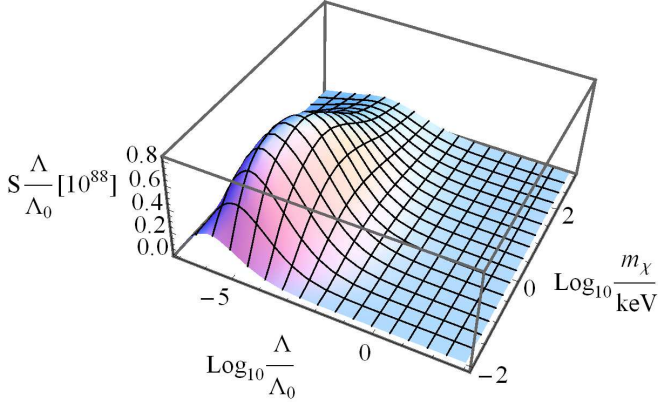


FIG. 16. Probability of observing a given value of the cosmological constant and mass of dark matter, assuming $g_s = \frac{m_\chi}{20\text{meV}}$, $\langle\sigma v\rangle = 3 \times 10^{-26} \frac{\text{cm}^3}{\text{s}}$, and that dark matter annihilation is the only contributor to entropy production in the causal diamond. This plot assumes the dark matter annihilates into photons which are scattered by dust at energies of 20 meV.

matter is favored by the causal entropic principle, if we assume that the prior on entropy per annihilation has only moderate dependence on the mass of the dark matter particle. (We discuss in Sect. I the relationship to current hints of possible observed dark matter annihilations.) Second, since annihilation will peak in the far future, a smaller value of the cosmological constant is favored (when annihilations dominate entropy production), on the order of 10^{-5} of the value $\Omega_\Lambda \approx 0.68$ measured today. Third, dark matter annihilations might produce a great deal of entropy within the causal diamond, pos-

sibly even greater than the entropy produced from dust heated by stars. In general the competition between en-

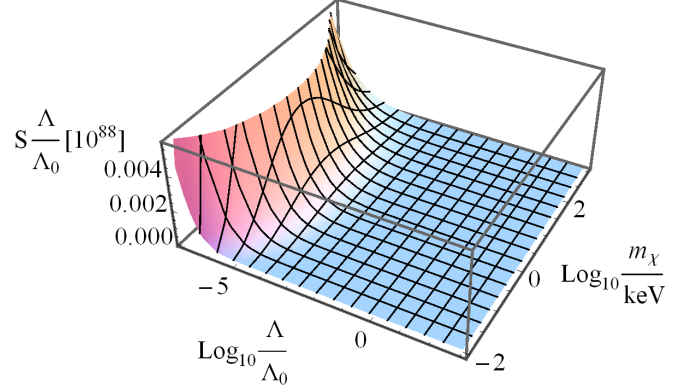


FIG. 17. Probability of observing a given value of the cosmological constant and mass of dark matter, assuming $g_s = \frac{m_\chi}{20\text{meV}}$, $\langle\sigma v\rangle = 3 \times 10^{-25} \frac{\text{cm}^3}{\text{s}}$, and that dark matter annihilation is the only contributor to entropy production in the causal diamond. This plot assumes the dark matter annihilates into photons which are scattered by dust at energies of 20 meV.

trophy from dark matter annihilations and from stars results in a bimodal probability distribution for Λ , not a single peak that might be “tuned” by these competing effects. In order for dark matter annihilation to dominate entropy production we need to have a large amount of entropy produced per particle decay and a moderately light dark matter particle.

We also have shown that using the causal entropic principle on the entropy from stars by varying the cross section for dark matter annihilation produces better agreement with observations than varying either the baryon fraction or the total matter abundance independently, as done in [4].

Furthermore, we have explored the effect of varying the cross section for dark matter annihilation, and found that the increase in matter density in the early universe resulting from a lowered cross section causes the dark matter to annihilate earlier, allowing a larger value of cosmological constant. This scenario is preferred by the causal entropic principle, and could in principle exhibit runaway behavior, as suggested in [13].

ACKNOWLEDGMENTS

We thank M. Bradač and D. Phillips for helpful conversations. One of us (AA) would like to thank the Kavli Institute for Theoretic Physics at UCSB for hospitality while this work was completed. This work was supported in part by DOE Grant DE-FG02-91ER40674 and the National Science Foundation under Grant No. PHY11-25915.

-
- [1] S. Weinberg, Phys.Rev.Lett. **59**, 2607 (1987).
- [2] R. Bouusso and J. Polchinski, JHEP **06**, 006 (2000), hep-th/0004134.
- [3] R. Bouusso, R. Harnik, G. D. Kribs, and G. Perez, Phys.Rev. **D76**, 043513 (2007), arXiv:hep-th/0702115 [hep-th].
- [4] J. M. Cline, A. R. Frey, and G. Holder, Phys.Rev. **D77**, 063520 (2008), arXiv:0709.4443 [hep-th].
- [5] B. Bozek, A. Albrecht, and D. Phillips, Phys.Rev. **D80**, 023527 (2009), arXiv:0902.1171 [astro-ph.CO].
- [6] D. Phillips and A. Albrecht, Phys.Rev. **D84**, 123530 (2011), arXiv:0903.1622 [gr-qc].
- [7] R. Bouusso, B. Freivogel, S. Leichenauer, and V. Rosenhaus, Phys.Rev. **D84**, 083517 (2011), arXiv:1012.2869 [hep-th].
- [8] R. Bouusso, B. Freivogel, S. Leichenauer, and V. Rosenhaus, Phys.Rev.Lett. **106**, 101301 (2011), arXiv:1011.0714 [hep-th].
- [9] R. Bouusso and R. Harnik, Phys.Rev. **D82**, 123523 (2010), arXiv:1001.1155 [hep-th].
- [10] R. Bouusso and S. Leichenauer, Phys.Rev. **D81**, 063524 (2010), arXiv:0907.4917 [hep-th].
- [11] B. Feldstein, L. J. Hall, and T. Watari, Phys.Rev. **D72**, 123506 (2005), arXiv:hep-th/0506235 [hep-th].
- [12] J. Garriga and A. Vilenkin, Prog.Theor.Phys.Suppl. **163**, 245 (2006), arXiv:hep-th/0508005 [hep-th].
- [13] I. Maor, T. W. Kephart, L. M. Krauss, Y. J. Ng, and G. D. Starkman, ArXiv e-prints (2008), arXiv:0812.1015 [hep-th].
- [14] L. Mersini-Houghton and F. C. Adams, Class.Quant.Grav. **25**, 165002 (2008), arXiv:0810.4914 [gr-qc].
- [15] M. P. Salem, Phys.Rev. **D80**, 023502 (2009), arXiv:0902.4485 [hep-th].
- [16] T. Bringmann and C. Weniger, Phys.Dark Univ. **1**, 194 (2012), arXiv:1208.5481 [hep-ph].
- [17] O. Adriani *et al.* (PAMELA Collaboration), Nature **458**, 607 (2009), arXiv:0810.4995 [astro-ph].
- [18] J. Chang, J. Adams, H. Ahn, G. Bashindzhagyan, M. Christl, *et al.*, Nature **456**, 362 (2008).
- [19] The Fermi-LAT Collaboration, Physical Review **D88**, 082002 (2013), arXiv:1305.5597 [astro-ph.HE].
- [20] H.-B. Jin, Y.-L. Wu, and Y.-F. Zhou, JCAP **1311**, 026 (2013), arXiv:1304.1997 [hep-ph].
- [21] D. H. Weinberg, J. S. Bullock, F. Governato, R. K. de Naray, and A. H. G. Peter, ArXiv e-prints (2013), arXiv:1306.0913 [astro-ph.CO].
- [22] J. E. Taylor and J. Silk, Mon.Not.Roy.Astron.Soc. **339**, 505 (2003), arXiv:astro-ph/0207299 [astro-ph].
- [23] P. Ade *et al.* (Planck Collaboration), ArXiv e-prints (2013), arXiv:1303.5076 [astro-ph.CO].
- [24] A. R. Zentner and J. S. Bullock, Astrophys.J. **598**, 49 (2003), arXiv:astro-ph/0304292 [astro-ph].
- [25] J. M. Bardeen, J. Bond, N. Kaiser, and A. Szalay, Astrophys.J. **304**, 15 (1986).
- [26] M. Tegmark, A. Aguirre, M. J. Rees, and F. Wilczek, Phys.Rev. **D73**, 023505 (2006), arXiv:astro-ph/0511774 [astro-ph].
- [27] J. F. Navarro, C. S. Frenk, and S. D. White, Astrophys.J. **490**, 493 (1997), arXiv:astro-ph/9611107 [astro-ph].
- [28] J. S. Bullock, T. S. Kolatt, Y. Sigad, R. S. Somerville, A. V. Kravtsov, *et al.*, Mon.Not.Roy.Astron.Soc. **321**, 559 (2001), arXiv:astro-ph/9908159 [astro-ph].
- [29] K. Dolag, M. Bartelmann, F. Perrotta, C. Baccigalupi, L. Moscardini, *et al.*, Astron.Astrophys. **416**, 853 (2004), arXiv:astro-ph/0309771 [astro-ph].
- [30] J. E. Gunn and I. Gott, J. Richard, Astrophys.J. **176**, 1 (1972).
- [31] R. K. Sheth, H. Mo, and G. Tormen, Mon.Not.Roy.Astron.Soc. **323**, 1 (2001), arXiv:astro-ph/9907024 [astro-ph].
- [32] R. M. Dunstan, K. N. Abazajian, E. Polisensky, and M. Ricotti, ArXiv e-prints (2011), arXiv:1109.6291 [astro-ph.CO].
- [33] R. E. Angulo, O. Hahn, and T. Abel, Mon.Not.Roy.Astron.Soc. **434**, 3337 (2013), arXiv:1304.2406 [astro-ph.CO].
- [34] A. Schneider, R. E. Smith, and D. Reed, Mon.Not.Roy.Astron.Soc. **433**, 1573 (2013), arXiv:1303.0839 [astro-ph.CO].
- [35] P. Gondolo and G. Gelmini, Nucl.Phys. **B360**, 145 (1991).
- [36] L. Hernquist and V. Springel, Mon.Not.Roy.Astron.Soc. **341**, 1253 (2003), arXiv:astro-ph/0209183 [astro-ph].